Gaussian Decomposition of Absorption and Linear Dichroism Spectra of Outer Antenna Complexes of Photosystem II

Giuseppe Zucchelli,*,‡ Paola Dainese,§ Robert C. Jennings,‡ Jacques Breton,∥ Flavio M. Garlaschi,‡ and Roberto Bassi⊥

Centro CNR Biologia Cellulare e Molecolare delle Piante, Dipartimento di Biologia, Università di Milano, via Celoria 26, 20133 Milano, Italy, Dipartimento di Biologia, Università di Padova, via Trieste 75, 35121 Padova, Italy, Commissariat a l'Energie Atomique, DBCM/Section de Bioenergetique, Bât.532, CE. Saclay, 91191 Gif-sur-Yvette Cedex, France, and Biotecnologie Vegetali, Università di Verona, strada Le Grazie 5, 37100 Verona, Italy

Received December 9, 1993; Revised Manuscript Received May 10, 1994®

ABSTRACT: Room temperature and 10 K absorption and linear dichroism spectra of the chlorophyll–protein complexes comprising the outer antenna of PSII (LHCII, CP29, CP26, CP24) have been analyzed in terms of a linear combination of asymmetric Gaussian bands. The results demonstrate the following: (a) The absorption and linear dichroism spectra of each sample can be described by nearly the same set of Gaussian bands at room temperature and 10 K. (b) The relative distributions of the transition moments of the major red-absorbing spectral forms seem to be similar in all four outer antenna chlorophyll–protein complexes at room temperature, with the 684-nm band being oriented closest to the particle plane at room temperature and the 677- and 669-nm bands being tilted at progressively greater angles out of the particle plane. The shorter wavelength transitions seem to be oriented close to the magic angle, but interpretation is complicated in this spectral region due to the low linear dichroism values and by overlap with vibrational bands. (c) The 684-nm band, detected in room temperature absorption and linear dichroism spectra of all complexes, vanishes at 10 K.

In photosynthesis, light is absorbed by a large array of antenna pigments which, in the case of higher plant photosystems, are mainly chlorophyll molecules. Photosystem II antenna contains about 200–250 chl[1] molecules for every reaction center (Anderson, 1986; Glazer & Melis, 1987). Excitation energy is transferred from the antenna to reaction centers where photochemical trapping occurs within about 300 ps after photon absorption (Leibl et al., 1989). Average chl–chl pairwise transfer rates are probably of the order of 1 ps (Jennings et al., 1993a), though a rather large spread of transfer rates is suggested by crystallographic studies for the principal PSII antenna complex, LHCII, in which nearest neighbor center–center distances are in the range 0.9–1.4 nm (Kühlbrandt & Wang, 1991). While the planes of the chlorophyll porphyrin rings of this complex were shown to be oriented at about 90° to the membrane plane (Kühlbrandt & Wang, 1991), the transition dipole orientations of the single chlorophylls are not yet known.

The antenna system of PSII consists of six different chl–protein complexes. Two of these, CP43 and CP47, which bind only chl *a*, are closely associated with the reaction center complex and are collectively known as the inner antenna. The other four complexes (LHCII, CP29, CP26, CP24), all of which contain chl *b* in addition to chl *a*, form the so-called outer antenna. On the basis of biochemical studies several structural models have been presented which describe the topological relations between these complexes in the PSII antenna (Peter & Thornber, 1991; Harrison & Melis, 1992; Dainese et al., 1992; Jansson, 1992).

The absorption spectrum of PSII antenna, as is the case also for PSI antenna, is modified by a coarse-grained inhomogeneous broadening associated with the presence of a number of different chl electronic transitions (Hayes et al., 1988; Ikegami & Itoh, 1988; Gillie et al., 1989; Zucchelli et al., 1990; Vacha et al., 1991; Van der Vos et al., 1991; Hemelrijk et al., 1992). One way which is commonly used to analyze this is that of spectral decomposition into Gaussian sub-bands (French et al., 1972; van Dorssen et al., 1987b; Ikegami & Itoh, 1988; Zucchelli et al., 1990, 1992; Van der Vos et al., 1991; Hemelrijk et al., 1992; Holzwarth, 1992; Jennings et al., 1993b; Trissl et al., 1993). For PSII, the absorption maxima for these sub-bands are commonly found at approximately 660, 670, 678, 685, and 695 nm. Chlorophyll *b*, which seems to be present as a single rather broad spectral band at RT, usually absorbs maximally near 648 nm (Zucchelli et al., 1990, 1992; Jennings et al., 1993b). It has recently been demonstrated that the chl *a* spectral forms, as revealed by Gaussian sub-bands analysis, are all present in each antenna complex in rather similar amounts (Jennings et al., 1993b). As most antenna complexes bind a number of chl *a* molecules which is greater than the detected number of spectral bands, it seems likely that at least some of the Gaussian spectral forms are site inhomogeneously broadened (see Discussion for further elaboration on this point).

It has been known for many years, on the basis of linear dichroism studies, that there are significant differences in orientation of the $Q_y(0,0)$ transition across the absorption band of thylakoids. From the earlier literature (Breton & Vermeglio, 1982) the following general conclusions could be drawn. The long wavelength chl *a* forms ($\lambda > 676$ nm) have their Q_y transition dipoles lying fairly close to the membrane plane, while the shorter wavelength chl *a* forms are closer to

‡ Università di Milano.
§ Università di Padova.
∥ Commissariat a l'Energie Atomique.
⊥ Università di Verona.

® Abstract published in *Advance ACS Abstracts,* July 1, 1994.

[1] Abbreviations: A, absorption; chl, chlorophyll; CP, chlorophyll–protein complex; DM, dodecyl maltoside; FWHM, full width at half-maximum; HWHM, half width at half-maximum; LD, linear dichroism; LHCII, light-harvesting chlorophyll *a*/*b* protein complex II; PSII, photosystem II; RT, room temperature.

0006-2960/94/0433-8982$04.50/0

35° out of the membrane plane. Most chl *b* is thought to be oriented at angles greater than 35° out of the membrane plane. More recently this picture has been confirmed for some antenna complexes of both photosystems (Haworth et al., 1982a; Tapie et al., 1986; Breton & Katoh, 1987; van Dorssen et al., 1987a,b; Breton, 1990; Hemelrijk et al., 1992; Kwa et al., 1992), though to date no LD measurements have been published on the three minor chl *a*/*b* complexes of the external antenna of PSII (CP29, CP26, CP24). In the present paper we present LD and absorption spectra measurements for the Q_y absorption band of these three complexes in addition to those for the major antenna pigment protein complex LHCII. As absorption and LD spectra are the sum of a number of overlapping bands, in order to determine the relative dichroic ratio (LD/A) of the spectral forms, both LD and absorption spectra have been decomposed by asymmetric Gaussian band analysis. Spectra were measured at both 300 and 10 K in order to determine whether temperature-induced changes occur since previous absorption analyses suggest that the 684-nm chl *a* form disappears at cryogenic temperatures in LHCII (Zucchelli et al., 1990). The data show that room temperature linear dichroism spectra of the four antenna complexes can be decomposed by a similar set of long wavelength Gaussian bands (670, 678, and 684 nm) as absorption spectra, thus demonstrating that each of these spectral forms displays considerable orientational homogeneity. The relative dichroic ratios, calculated by assuming the maximum values for the LD/3A parameter for the dipole vector associated with the 684-nm transition, are similar for each of these three long wavelength forms in all four outer antenna complexes. It is also shown that the long wavelength spectral form with a maximum at 684 nm is absent at cryogenic temperature in all four pigment–protein complexes examined.

MATERIALS AND METHODS

Preparation of Thylakoid Membranes. Seedlings of *Zea mays* (cv Dekalb DF28) were grown for 2–3 weeks in a growth chamber at 12/12 h light/dark and 28/21 °C day/night at a light intensity of 10 000 lx and 80% humidity. Leaves from 2–3-week-old plants were harvested at the end of a 12-h dark period, and thylakoids from mesophyll chloroplasts were obtained as previously described (Bassi & Simpson, 1986). PSII membranes were prepared according to the method of Berthold et al. (1981), using the modifications described by Dunahay et al. (1984). Aliquots were resuspended at 3 mg of chl/mL in 25 mM Hepes, pH 7.6, 5 mM $MgCl_2$, 10 mM NaCl, and 0.2 M sorbitol and frozen at −80 °C until required.

Sucrose Gradient Ultracentrifugation. PSII membranes were washed twice in 1 mM EDTA, pH 8.0, then resuspended in water at 2 mg of chl/mL, and solubilized by adding an equal volume of 2% DM in water. When required, other detergent concentrations were used or $MgCl_2$ was added to a final concentration of 5 mM, in both the solubilization mixture and the sucrose gradient. The solubilized sample was spun for 2 min at 15000*g* at 4 °C and then rapidly loaded onto a 0.1–1.0 M sucrose gradient containing 10 mM Hepes, pH 7.6, and 0.06% DM. The gradient was then spun on a Beckman SW41 rotor at 39 000 rpm for 23 h at 4 °C. For quantitative determinations, the gradient was fractionated from the top into 250-μL aliquots.

Purification of chl a/b Binding Proteins. Purified LHCII, CP29, CP26, and CP24 were obtained as previously reported (Dainese et al., 1990; Bassi & Dainese, 1992; Dainese & Bassi, 1991).

Spectroscopic Analysis. The 300 and 10 K absorption and linear dichroism spectra of the isolated chl *a*/*b* protein complexes have been measured as described by Haworth et al. (1982b) using samples oriented by the polyacrylamide gel squeezing technique. The instrumental bandwidth was 2 nm.

The normalized linear dichroism spectra have been analyzed in terms of the orientation parameter LD/3A (Breton et al., 1973) defined by

$$\frac{LD}{3A} = \frac{A_{\parallel} - A_{\perp}}{3A} = \frac{1 - 3\cos^2 \Phi}{2} \quad (1)$$

where A is the absorption spectrum of the sample, $A_{\parallel}$ and $A_{\perp}$ are respectively the absorption spectra obtained with light polarized parallel or perpendicular with respect to the plane of gel stretching, and Φ is the angle between the dipole vector and the normal to this plane. The ratio (1) is difficult to interpret when the absorption and LD spectra are of a composite nature. The decomposition of both spectra as sub-bands gives the possibility to analyze separately the contribution due to each absorption band. In order to compare the relative transition dipole orientations of the spectral forms, we have arbitrarily assigned values of LD/3A = 0.5 for the sub-band having the greatest LD/A ratio in the normalized spectra. The other bands are normalized accordingly.

Curve Fitting. Decomposition analyses of the spectra in terms of asymmetric Gaussian bands have been performed as already described (Jennings et al., 1993b) using a nonlinear least-squares algorithm that minimizes the χ^2 functions with respect to a model function. This model function is a linear combination of a number of Gaussian bands given as input parameters. A maximum number of 20 bands is allowed, and each band is defined by its wavelength position, amplitude, and two HWHM values, the right and the left one. All of these parameters were left free in all of the fits performed. Negative values of the amplitude are numerically allowed. The choice of a Gaussian model is physically well founded for analysis of the absorption spectra (see Discussion), and the allowed asymmetry can model possible effects of linear electron coupling with vibrational modes of the system (Champion & Albrecht, 1980; Chan & Page, 1983). The same model can, in principle, also be used to analyze LD spectra, provided each Gaussian sub-band represents a single dipole orientation. In this case the band shape of the LD decomposition Gaussians is a function only of the absorption bands (eq 1).

RESULTS

In Figures 1–4 the absorption and linear dichroism spectra of the four pigment–protein complexes comprising the outer antenna of PSII (LHCII, CP29, CP26, CP24) are presented for the wavelength range 630–720 nm. Spectra were determined at both 300 and 10 K. The room temperature absorption spectra are similar to those previously reported for these complexes (Jennings et al., 1993b), as is the corresponding low-temperature spectrum for LHCII (Hemelrijk et al., 1992; Kwa et al., 1992). Lowering the temperature results in narrowing of the absorption spectra which is markedly asymmetric toward longer wavelengths, as has already been described for LHCII by moments analysis (Zucchelli et al., 1990). Significant (1–3 nm) blue shifts of the peak values are also observed for all complexes at 10 K. LD spectra can be seen to be positive in all complexes for wavelengths greater than 660–665 nm at both temperatures used in the analysis. The signal goes to zero or oscillates around zero in the wavelength region shorter than 660 nm. The positive LD signals are due to chl *a* Q_y absorption, while

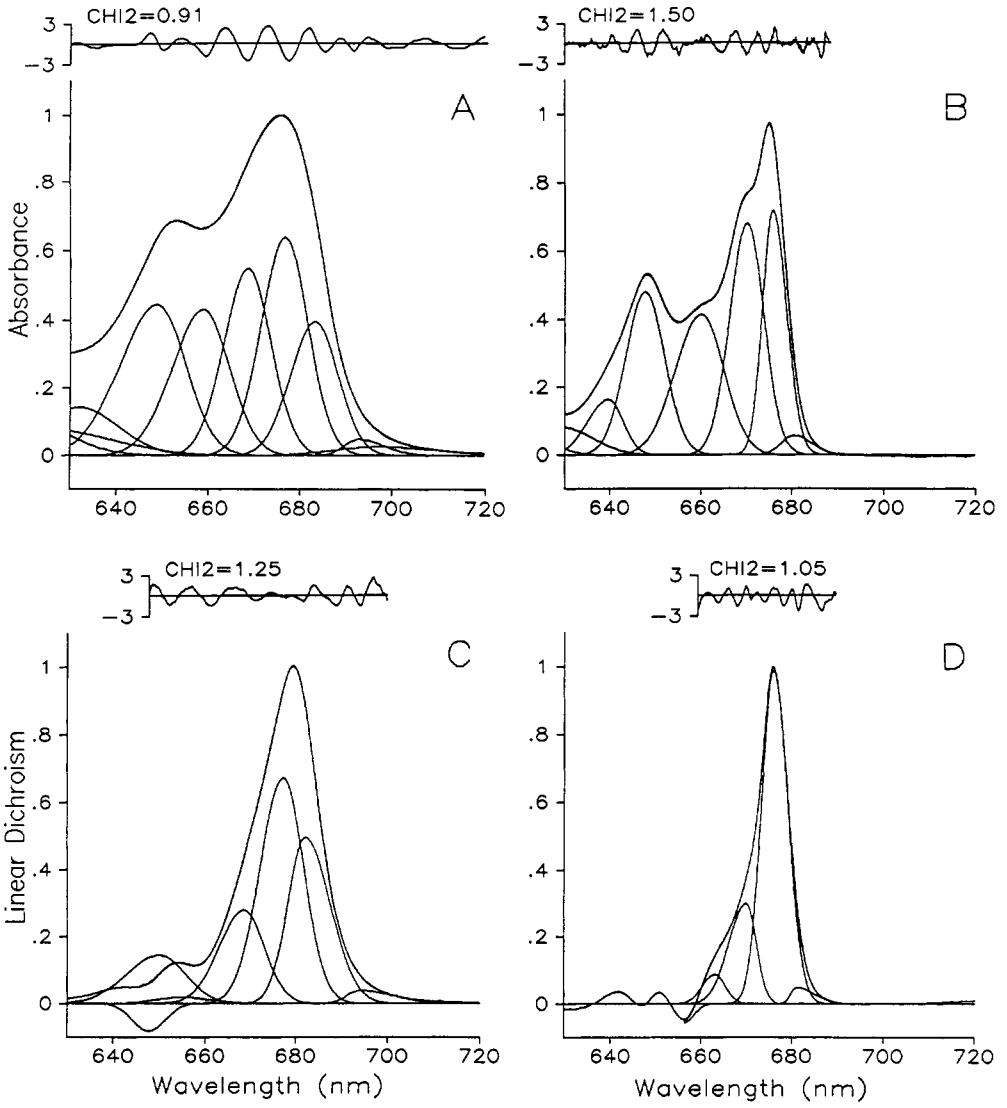

FIGURE 1: Asymmetric Gaussian band decomposition of absorption and linear dichroism spectra of LHCII measured at 300 (A, C) and 10 K (B, D). The residuals and the χ^2 values are also shown and used to judge the goodness of the fits. The width of the residual plot gives the spectral wavelength interval analyzed.

in the chl *b* Q_y region (~650 nm) the LD signals are slightly negative or close to zero. These data for LHCII are in good agreement with previously published LD measurements performed at cryogenic temperatures (Hemelrijk et al., 1992; Kwa et al., 1992; Haworth et al., 1982a). In all cases lowering the temperature led to marked narrowing of LD spectra with significant blue shifting (3–5 nm) of the peak value.

Previous results have shown that room temperature absorption spectra of all four outer antenna complexes are well described by a linear sum of essentially the same five main Gaussian bands with the wavelength position of maxima between 648 and 684 nm (Jennings et al., 1993b). Calculation of the errors associated with each spectral parameter indicated the uniqueness of these fits (see Discussion for some remarks about the use of a Gaussian model). This result is confirmed here (Figures 1–4; Tables 1–4). For all complexes the absorption spectra at low temperature can be described by Gaussians with similar peak value wavelength positions, with the exception of the 684-nm band. This band almost disappears in the low-temperature analysis. A similar result has already been published for isolated LHCII (Zucchelli et al., 1990). Preliminary studies with LHCII indicate that this temperature effect is reversible. For the 677-nm band significant decreases in intensity for CP24 and CP26 at 10 K were also detected, while this remained almost constant in CP29 and LHCII. The decrease in long wavelength band intensity at 10 K is accompanied by intensity increases in the shorter wavelength Gaussians, thus suggesting a temperature-sensitive redistribution of transition moments within these isolated complexes. This conclusion is supported by analysis of the effect of temperature on bandwidth. In all complexes this parameter shows a marked decrease for the 677-nm Gaussian at 10 K. The shorter wavelength Gaussians, however, display less apparent temperature sensitivity with the exception of CP29 where significant short wavelength band narrowing was detected. This exception is significant as the low-temperature decrease in long wavelength band intensity in CP29 is less marked than in the other complexes. Thus a correlation exists between the short wavelength band narrowing at 10 K and the intensity decrease of long-wavelength bands. It is therefore reasonable to suggest that the long-wavelength transitions, which disappear at low temperatures, become associated with the shorter wavelength Gaussians, thus increasing their site inhomogeneous bandwidth.

In LHCII, CP24, and CP26 the broad Gaussian peaking near 650 nm in the RT spectra is associated with chl *b*. In CP29 the chl *b* Gaussian is considerably blue shifted, as previously reported (Jennings et al., 1993b). At 10 K,

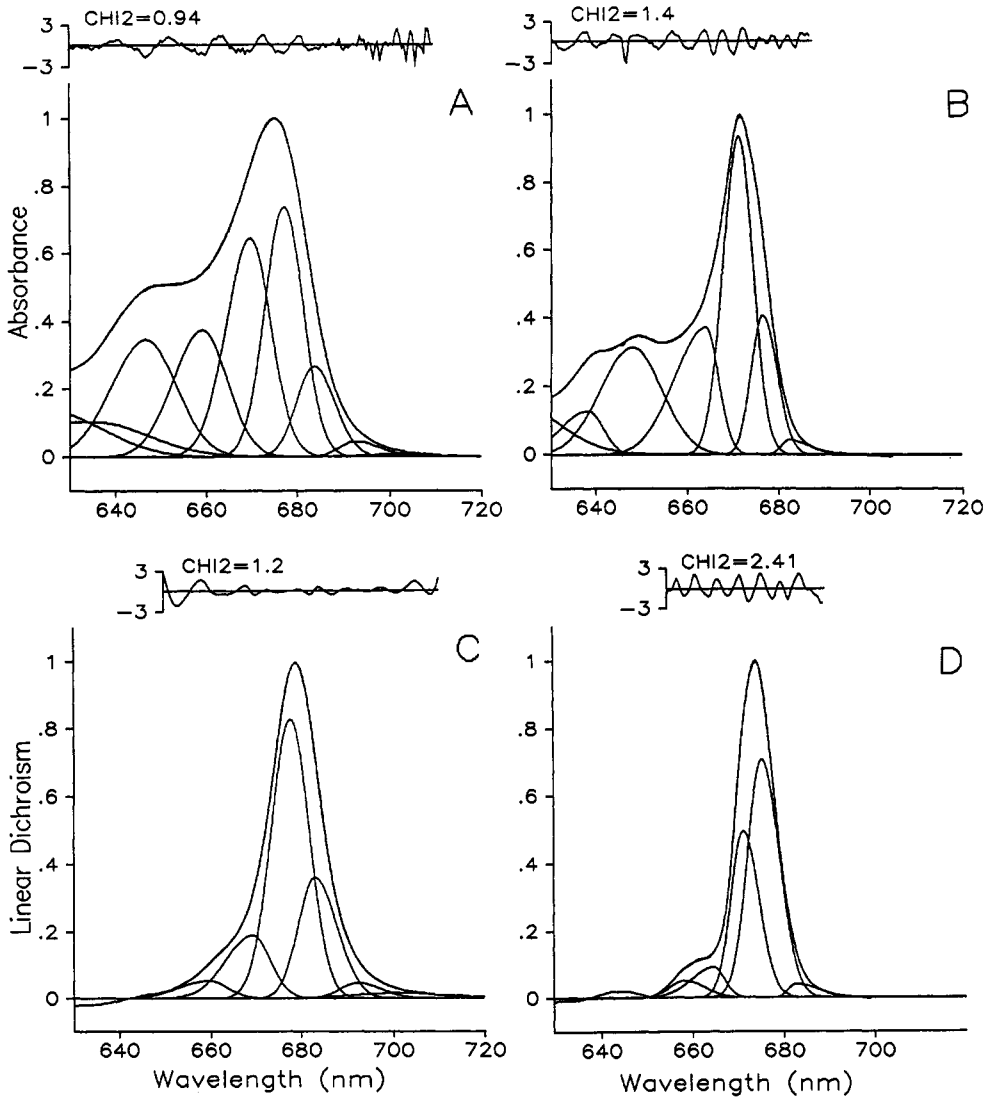

FIGURE 2: Asymmetric Gaussian band decomposition of absorption and linear dichroism spectra of CP24 measured at 300 (A, C) and 10 K (B, D). The residuals and the χ^2 values are also shown and used to judge the goodness of the fits. The width of the residual plot gives the spectral wavelength interval analyzed.

decomposition of all of the chl–protein absorption spectra shows two Gaussians, near 640 and 650 nm. This suggests the possibility of two distinguishable transitions associated with chl *b* that merge at RT due to the broadening and perhaps a shift of the bands. In this region the numerical analysis is complicated by the presence of a nearly flat and unstructured zone of the absorption spectrum at RT.

The positive region of the LD spectra can be well described, at both temperatures, by nearly the same Gaussian bands used to fit the corresponding absorption spectra in all complexes, though some minor differences are observed (Figures 1–4; Tables 1–4). In particular, the match between LD and absorption is not very close in the long-wavelength tail ($\lambda > 690$ nm). As this region is subject to large experimental errors, interpretation is difficult, and we do not attribute any particular physical meaning to these minor bands. The rather close correspondence for the three major sub-bands, however, suggests that these absorption bands are to a first approximation orientationally homogeneous (see Materials and Methods). The small differences in bandwidth and position encountered may indicate minor orientational differences associated with different electronic transitions in each site inhomogeneously broadened sub-bands (see Discussion). For transition dipoles oriented close to the particle plane, small differences (<10–15°) in orientation of different chromophores contributing to each spectral band are not expected to significantly alter the linear dichroism decompositions as these would lead to only minor differences (<10%) in the orientation parameter (Breton & Vermeglio, 1982). For dipole orientations at greater angles to the particle plane, differences between chromophores in any one Gaussian band would be considerably less than 10°. These data therefore lend strong support to the physical significance of these Gaussian decompositions.

In the wavelength region below 660 nm the LD signal at room temperature is small and at 10 K oscillates around zero. Here the sub-band LD analysis does not resemble that for absorption spectra. Exact interpretation of this is impossible as several factors may be involved: (a) low signal to noise ratio and base line correction uncertainties, (b) orientational dishomogeneity of a number of strongly overlapping chl *b* Q_y transitions which are not resolved by the present analysis, or (c) presence of vibrational bands of the long wavelength chl *a* forms. The LD–Gaussian curves shown in Figures 1–4 in the wavelength region below 660 nm are therefore not considered to have physical significance.

For all the chl–protein complexes, the RT linear dichroism spectra are described by three major positive sub-band contributions. The main Gaussian is always associated with

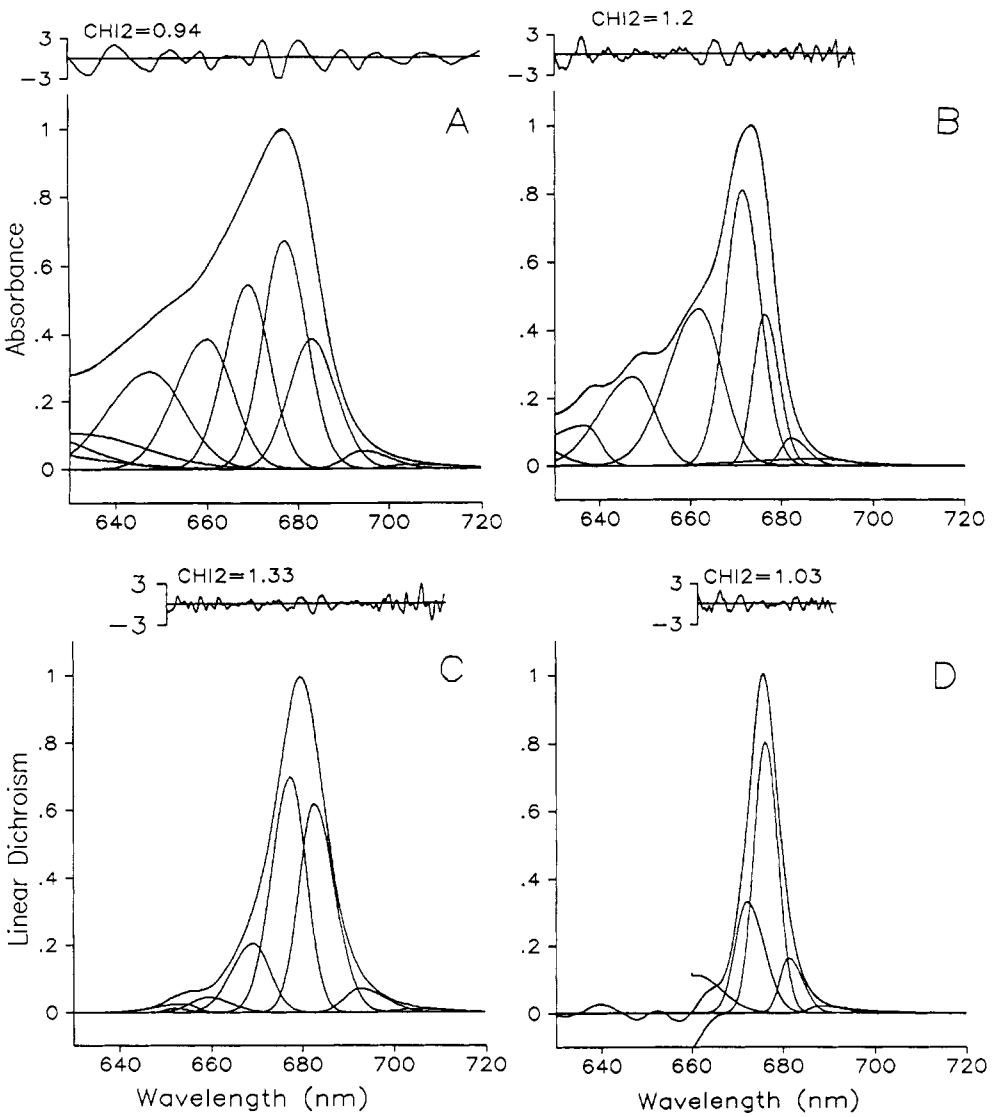

FIGURE 3: Asymmetric Gaussian band decomposition of absorption and linear dichroism spectra of CP26 measured at 300 (A, C) and 10 K (B, D). The residuals and the χ^2 values are also shown and used to judge the goodness of the fits. The width of the residual plot gives the spectral wavelength interval analyzed.

the 677-nm band followed by contributions due to the 684-nm band and the 670-nm band. At low temperature, however, the positive LD signal is, in all the complexes examined, substantially dominated by two bands as the 684-nm LD Gaussian is greatly reduced. The principal contribution is in all cases due to the 677-nm band with the extreme case of CP29 where this band is over 80% of the positive LD spectrum.

In order to obtain information on the relative orientation of transition dipoles, the parameter LD/3A (eq 1) has been calculated for the three major long-wavelength bands in each complex from the room temperature spectral decompositions (see Materials and Methods). As this parameter is greatest for the 684-nm band in all complexes, we have assumed an LD/3A value of 0.5 for it and have normalized the other bands to this value (Table 5). From this analysis the relative distribution of the transition moments of the different spectral forms is expected to be substantially equal in all four outer antenna complexes. The 684-nm transitions lie closest to the particle plane, while the 677-nm and 669-nm transitions are oriented at progressively greater angles out of the particle plane toward the magic angle ($\sim$35° with respect to the particle plane). In the wavelength region around 650 nm, where chl *b* has its absorption maximum in most complexes, the LD values go rapidly to zero or are negative. This may indicate that the chl *b* transition moment lies at an angle equal to or slightly lower than the magic angle. However, the possibility cannot be excluded that the LD signal in the wavelength region below 670 nm comes from a positive contribution due to the 660-nm absorption band and a negative contribution by the chl *b* band, higher than that estimated directly from the LD spectra.

DISCUSSION

In the present paper the absorption and linear dichroism spectra of all of the chl–protein complexes comprising the external antenna of PSII, measured at both RT and 10 K, have been analyzed in terms of a linear combination of asymmetric Gaussian bands. It is demonstrated that both absorption and LD spectra of the same sample at the same temperature can be well described by similar Gaussian bands in the wavelength range 660–690 nm. This observation gives strong support to the use of a linear combination of Gaussian bands as a model for describing the coarse-grained inhomogeneous nature of the Q_y absorption band of the complexes. We interpret each of these decomposition Gaussian bands as representing the homogeneously broadened absorption lines of closely lying electronic transitions (site inhomogeneous

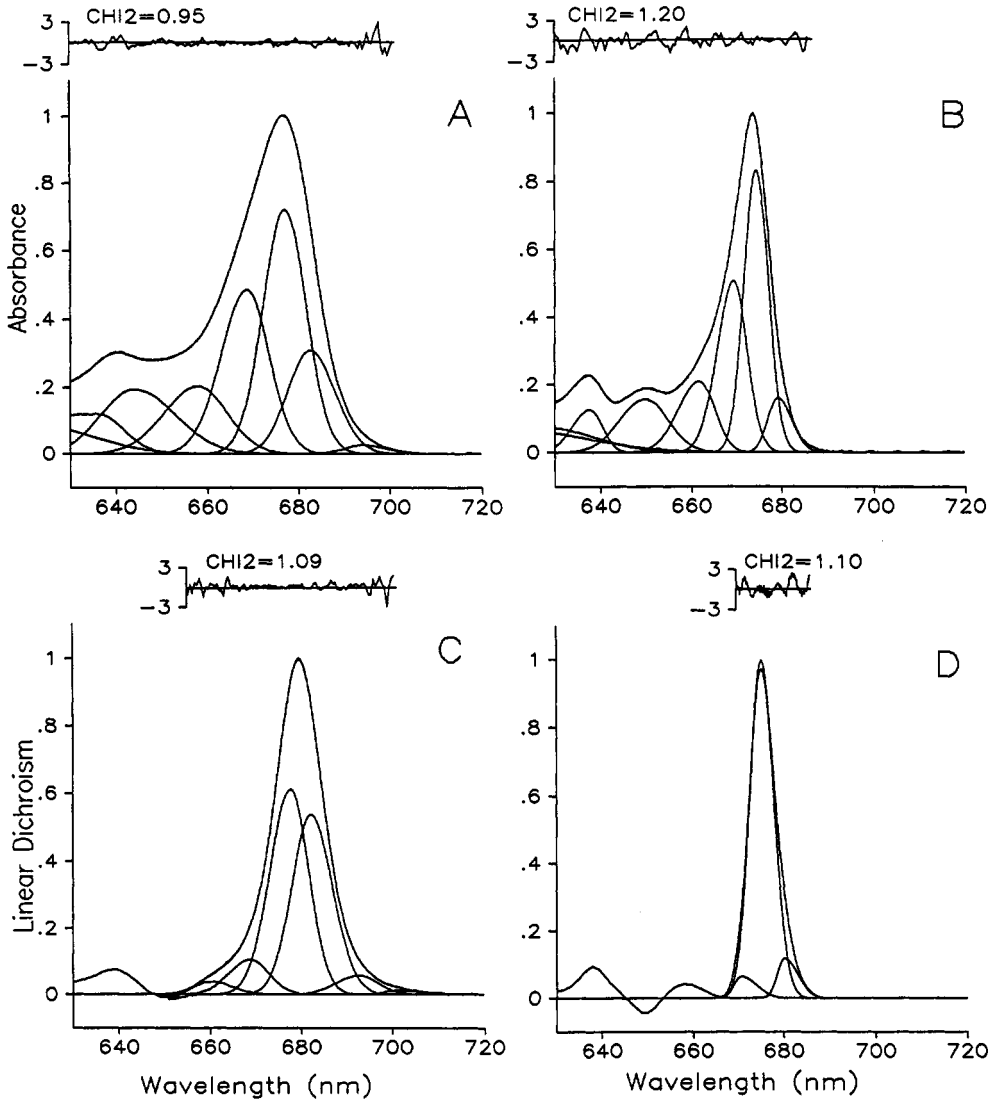

FIGURE 4: Asymmetric Gaussian band decomposition of absorption and linear dichroism spectra of CP29 measured at 300 (A, C) and 10 K (B, D). The residuals and the χ^2 values are also shown and used to judge the goodness of the fits. The width of the residual plot gives the spectral wavelength interval analyzed.

broadening). Thus the band width (Γ) of a spectral form may be defined, in the case of Gaussian bands, by

$$\Gamma^2 = \Gamma^2_{hom} + \Gamma^2_{inh} \quad (2)$$

In physical terms, the site inhomogeneous component may be conceived of either as slightly different protein binding sites for chromophores or as a distribution of protein conformational substates (Ormos et al., 1990).

Concerning the use of Gaussian bands to describe optical transitions, a few words are in order. The absorption band of a system can be described from the set of normal modes of vibration (Champion & Albrecht, 1980; Chan & Page, 1983; Di Pace et al., 1992). For a single electronic transition a widely used approach (Chan & Page, 1983; Di Pace et al., 1992) is to separate the entire set of normal modes into two subsets, one of high-frequency modes, responsible for the vibronic structure of the absorption spectrum that is described by a sum of Lorentzian curves with Poissonian weightings and is independent of temperature, and a second subset of low-frequency normal modes. The coupling with these latter modes gives a contribution to the absorption shape that is usually described by a Gaussian and is temperature dependent. The total homogeneous band is then analytically described as a convolution of the Lorentzian and Gaussian bands, a function known as Voigtian. The Gaussian terms usually dominate the spectral shape, especially at high temperature, so that the simple Gaussian form is a good physical description of a homogeneously broadened electronic transition. In the case of an additional inhomogeneous broadening component, this is usually represented as a convolution with a Gaussian distribution. The total band is then a Gaussian, the width of which is given by eq 2.

For all the pigment–protein complexes examined, a positive LD signal in the wavelength interval above 660–665 nm was detected at both 300 and 10 K. While it is not possible to determine absolute angular coefficients for the spectral forms, the analysis shows that their distribution seems to be similar in all complexes. Thus the transition dipole of the 684-nm band is oriented closest to the particle plane with the 677- and 669-nm bands being tilted at progressively greater angles. The shorter wavelength transitions seem to be oriented rather close to the magic angle ($\sim$35° with respect to the particle plane), though an exact interpretation here is not possible, as discussed in the Results section. These observations are referred to the particle plane. It is probable, however, that this is parallel to the membrane plane, due to hydrophobic interactions between complexes during gel polymerization.

Table 1: Gaussian Band Parameters for the Decomposition of Absorption and Linear Dichroism Spectra of LHCII Measured at 300 and 10 K[a]

	300 K		10 K	
	A	LD	A	LD
1 λ_{max}	649.0		648.5	
FWHM	17.0		10.0	
HWHM	9.5, 7.5		5.0, 5.0	
area (%)	22.3		23.1	
2 λ_{max}	659.5		661.0	663.5
FWHM	15.0		12.5	6.0
HWHM	8.0, 7.0		6.5, 6.0	3.0, 3.0
area (%)	19.1		24.6	5.3
3 λ_{max}	669.0	669.0	671.0	670.5
FWHM	12.0	12.0	9.0	7.0
HWHM	6.0, 6.0	6.5, 5.5	4.5, 4.5	4.5, 2.5
area (%)	19.9	19.7	28.8	21.9
4 λ_{max}	677.0	678.0	676.5	676.5
FWHM	12.0	11.5	6.0	6.5
HWHM	6.0, 6.0	6.0, 5.5	2.5, 3.5	3.0, 3.5
area (%)	22.8	45.3	21.4	69.7
5 λ_{max}	684.0	682.5	681.0	681.5
FWHM	12.0	11.0	7.5	6.5
HWHM	6.0, 6.0	4.5, 6.5	3.0, 4.5	1.5, 4.5
area (%)	14.4	32.2	2.2	3.1
6 λ_{max}	693.0	694.0		
FWHM	10.5	12.0		
HWHM	3.5, 7.0	3.0, 9.0		
area (%)	1.5	2.8		

[a] The percentage areas have been calculated from the total area given by the sum of all the bonds. The FWHM is given as the sum of a left and a right HWHM value, which are also included. All of the band parameters were left free in these fits.

Table 2: Gaussian Band Parameters for the Decomposition of Absorption and Linear Dichroism Spectra of CP24 Measured at 300 and 10 K[a]

	300 K		10 K	
	A	LD	A	LD
1 λ_{max}	647.0		648.5	
FWHM	17.0		15.5	
HWHM	9.0, 8.0		8.0, 7.5	
area (%)	20.1		25.6	
2 λ_{max}	659.5	660.0	664.5	665.0
FWHM	14.0	12.5	11.5	9.0
HWHM	7.5, 6.5	7.5, 5.0	8.0, 3.5	6.0, 3.0
area (%)	18.2	4.5	21.8	7.4
3 λ_{max}	670.5	669.5	671.5	672.0
FWHM	12.0	11.5	8.0	7.0
HWHM	6.5, 5.5	7.0, 4.5	4.0, 4.0	3.0, 4.0
area (%)	25.9	14.6	36.9	34.5
4 λ_{max}	678.0	678.0	677.0	676.0
FWHM	10.0	10.0	6.5	8.0
HWHM	5.0, 5.0	5.0, 5.0	3.0, 3.5	3.5, 4.5
area (%)	25.2	54.1	14.0	55.0
5 λ_{max}	684.5	683.5	683.0	683.0
FWHM	9.5	10.0	7.0	7.5
HWHM	4.5, 5.0	4.5, 5.5	2.0, 5.0	1.5, 6.0
area (%)	9.0	23.6	1.7	3.0
6 λ_{max}	693.0	692.5		
FWHM	10.5	10.5		
HWHM	4.0, 6.5	4.5, 6.0		
area (%)	1.6	3.3		

[a] For details, see Table 1.

Table 3: Gaussian Band Parameters for the Decomposition of Absorption and Linear Dichroism Spectra of CP26 Measured at 300 and 10 K[a]

	300 K		10 K	
	A	LD	A	LD
1 λ_{max}	648.0		648.0	
FWHM	19.5		14.5	
HWHM	11.5, 9.0		9.0, 5.5	
area (%)	18.2		17.4	
2 λ_{max}	660.5	660.0	662.5	
FWHM	14.5	11.0	14.0	
HWHM	8.0, 6.5	5.0, 6.0	8.0, 6.0	
area (%)	18.6	3.2	29.7	
3 λ_{max}	669.5	669.5	672.0	672.5
FWHM	11.5	10.0	9.0	7.5
HWHM	6.0, 5.5	5.5, 4.5	4.5, 4.5	3.0, 4.5
area (%)	20.6	13.3	34.2	28.9
4 λ_{max}	677.5	678.0	677.0	676.5
FWHM	11.5	9.0	6.5	6.0
HWHM	5.5, 6.0	5.0, 4.0	3.0, 3.5	3.0, 3.0
area (%)	25.0	40.9	13.6	57.6
5 λ_{max}	683.5	683.0	682.5	681.5
FWHM	12.5	9.5	7.0	5.5
HWHM	6.0, 6.5	4.0, 5.5	2.5, 4.5	2.0, 3.5
area (%)	15.6	37.7	2.5	11.2
6 λ_{max}	695.0	693.0	689.0	688.0
FWHM	11.5	10.5	26.5	9.0
HWHM	4.5, 7.0	4.0, 6.5	18.5, 8.0	2.5, 6.5
area (%)	2.0	4.9	2.6	2.3

[a] For details, see Table 1.

Table 4: Gaussian Band Parameters for the Decomposition of Absorption and Linear Dichroism Spectra of CP29 Measured at 300 and 10 K[a]

	300 K		10 K	
	A	LD	A	LD
1 λ_{max}			638.5	
FWHM			7.5	
HWHM			4.5, 3.0	
area (%)			6.4	
2 λ_{max}	644.5		650.5	
FWHM	19.0		12.5	
HWHM	8.5, 10.5		6.5, 6.0	
area (%)	14.4		12.9	
3 λ_{max}	658.5	661.0	662.5	
FWHM	16.5	10.5	9.5	
HWHM	9.0, 7.5	5.0, 5.5	5.5, 4.0	
area (%)	13.1	2.8	13.1	
4 λ_{max}	699.0	669.0	670.0	671.0
FWHM	13.0	10.5	8.0	6.0
HWHM	7.0, 6.0	5.5, 5.0	4.5, 3.5	2.0, 4.0
area (%)	24.1	7.7	26.3	5.4
5 λ_{max}	677.5	678.0	675.0	676.0
FWHM	11.0	10.5	6.0	6.0
HWHM	5.5, 5.5	5.5, 5.0	3.0, 3.0	3.0, 3.0
area (%)	32.1	44.3	34.9	86.0
6 λ_{max}	683.0	682.5	679.5	681.0
FWHM	12.5	10.5	6.0	5.5
HWHM	6.0, 6.5	5.0, 5.5	2.5, 3.5	2.0, 3.5
area (%)	15.0	40.7	6.4	8.7
7 λ_{max}	694.5	693.0		
FWHM	10.5	11.0		
HWHM	4.5, 6.0	6.0, 5.0		
area (%)	1.2	4.4		

[a] For details, see Table 1.

These data for the four outer antenna complexes are in general agreement with earlier LD measurements on LHCII at cryogenic temperatures (Kramer & Amesz, 1982; Hemelrijk et al., 1992; Kwa et al., 1992; Haworth et al., 1982a,b) and thylakoids (Breton et al., 1973; Haworth et al., 1982a,b), though previously a spectral band analysis was not attempted. In this respect it should be noted, however, that the present LD decomposition indicates for the first time that the 669-nm form has a positive LD signal. Previously it was suggested to be LD-silent and oriented very close to the magic angle (Hemelrijk et al., 1992; Kwa et al., 1992).

There is some disagreement in the literature on the red-most transitions in LHCII. Thus Kwa et al. (1992) on the basis of a detailed spectroscopic analysis at cryogenic temperatures conclude that the most red shifted spectral form

Table 5: Orientation Parameters LD/3A Calculated for Each Gaussian Band Describing RT Absorption Spectra of the chl–Protein Complexes Comprising the External Antenna of PSII[a]

	LD/3A			
λ_{max} (nm)	LHCII	CP29	CP26	CP24
669	0.22	0.06	0.13	0.11
677	0.44	0.25	0.34	0.41
684	0.50	0.50	0.50	0.50

[a] λ_{max} values are the approximate wavelength values of the maxima of the bands. LD/3A is defined in eq 1 (Materials and Methods) and has been calculated from the decomposition Gaussian area values.

peaks near 676 nm. On the other hand, Gaussian decomposition of absorption and fluorescence spectra at room temperature and 77 K suggests that a significant temperature-sensitive transition is present near 684 nm (Zucchelli et al., 1990). The latter interpretation is supported in the present study by the demonstration of a 684-nm Gaussian band in the LD spectrum at room temperature. Thus it is possible to clearly distinguish the orientation of the transition dipole associated with this band from those absorbing at shorter wavelengths. Consistent with previous observations (Zucchelli et al., 1990), this band is absent from both absorption and LD spectra at cryogenic temperature. It is interesting to note that this not only is a property of the long wavelength spectral form of LHCII but occurs analogously in all four outer antenna complexes. Analysis of the band intensities and bandwidths suggests that the red-shifted transitions at room temperature become redistributed at low temperatures among a number of shorter wavelength Gaussians. These observations therefore suggest that caution should be applied to interpretation of low-temperature spectroscopic data in antenna–protein complexes.

In recent years hole-burning spectroscopy has been performed using different chl–protein complex preparations (Gillie et al., 1987, 1989; Hayes et al., 1988; Tang et al., 1990). Values for the linear coupling coefficient, $S_1 \leq 0.9$, and the mean phonon frequency of the bath $\tilde{\nu}_1 \approx 22$–30 cm^{-1}, parameters involved in the temperature-sensitive vibrational broadening contribution, have been obtained. With these parameters it is possible to calculate the temperature-dependent contribution to the homogeneous bandwidth (in cm^{-1}) of an absorption band using (Hayes et al., 1988)

$$\mathrm{FWHM}^2 = (8 \ln 2) S_1 \tilde{\nu}_1^2 \coth(hc\tilde{\nu}_1)/(2k_B T) \qquad (3)$$

where h is the Planck constant, c is the velocity of light, k_B is the Boltzmann constant, and T is the temperature. A homogeneous bandwidth of about 200 cm^{-1} is thus estimated at RT, a value that gives FWHM in the range 9–11 nm. The FWHM values obtained by sub-band analysis are in the range 9.7–12.6 nm for the 684-, 677-, and 670-nm bands and around 14 nm for the 660-nm band (Tables 1–4), values that are comparable with those estimated above. The difference can be interpreted as due to the presence of an inhomogeneous contribution to the total bandwidth, which may also explain the small differences encountered between LD and absorption sub-bands. These observations lend further support to the sub-band description as a physically reasonable model to describe the absorption spectra of all the different chl–protein complexes.

ACKNOWLEDGMENT

We thank Dr. O. Cremonesi for the curve-fitting program.

REFERENCES

Anderson, J. M. (1986) *Annu. Rev. Plant Physiol. 37*, 93–136.
Bassi, R., & Simpson, D. J. (1986) *Carlsberg Res. Commun. 51*, 363–370.
Bassi, R., & Dainese, P. (1992) *Eur. J. Biochem. 204*, 317–326.
Berthold, D. A., Babcock, G. T., & Yocum, C. F. (1981) *FEBS Lett. 134*, 231–234.
Breton, J. (1990) in *Perspectives in Photosynthesis* (Jortner, J., & Pullman, B., Eds.) pp 23–38, Kluwer Academic Publishers, Dordrecht.
Breton, J., & Vermeglio, A. (1982) in *Photosynthesis, Energy conversion by plants and bacteria, Vol. 1* (Govindjee, Ed.), pp 153–194, Academic Press, New York.
Breton, J., & Katoh, S. (1987) *Biochim. Biophys. Acta 892*, 99–107.
Breton, J., Michel-Villaz, M., & Paillotin, G. (1973) *Biochim. Biophys. Acta 314*, 42–56.
Champion, P. M., & Albrecht, A. C. (1980) *J. Chem. Phys. 72*, 6498–6506.
Chan, C.-K., & Page, J. B. (1983) *J. Chem. Phys. 79*, 5234–5249.
Dainese, P., & Bassi, R. (1991) *J. Biol. Chem. 266*, 8136–8142.
Dainese, P., Hoyer-Hansen, G., & Bassi, R. (1990) *Photochem. Photobiol. 51*, 693–703.
Dainese, P., Santini, C., Ghiretti-Magaldi, A., Marquardt, J., Tidu, V., Mauro, S., Bergantino, E., & Bassi, R. (1992) in *Research in Photosynthesis, Vol. 2* (Murata, N., Ed.) pp 13–20, Kluwer Academic Publishers, Dordrecht, Boston, London.
Di Pace, A., Cupane, A., Leone, M., Vitrano, E., & Cordone, L. (1992) *Biophys. J. 63*, 475–484.
Dunahay, T. G., Staehelin, L. A., Seibert, M., Ogilvie, P. D., & Berg, S. P. (1984) *Biochim. Biophys. Acta 764*, 170–193.
French, C. S., Brown, J. S., & Lawrence, M. C. (1972) *Plant Physiol. 49*, 421–429.
Gillie, J. K., Hayes, J. M., Small, G. J., & Golbeck, J. H. (1987) *J. Phys. Chem. 91*, 5524–5527.
Gillie, J. K., Small, G. J., & Golbeck, J. H. (1989) *J. Phys. Chem. 93*, 1620–1627.
Glazer, A. N., & Melis, A. (1987) *Annu. Rev. Plant Physiol. 38*, 11–45.
Harrison, M. A., & Melis, A. (1992) *Plant Cell Physiol. 33*, 627–637.
Haworth, P., Tapie, P., Arntzen, C. J., & Breton, J. (1982a) *Biochim. Biophys. Acta 682*, 504–506.
Haworth, P., Arntzen, C. J., Tapie, P., & Breton, J. (1982b) *Biochim. Biophys. Acta 682*, 152–159.
Hayes, J. M., Gillie, J. K., Tang, D., & Small, G. J. (1988) *Biochim. Biophys. Acta 932*, 287–305.
Hemelrijk, P. W., Kwa, S. L. S., van Grondelle, R., & Dekker, J. P. (1992) *Biochim. Biophys. Acta 1098*, 159–166.
Holzwarth, A. R. (1992) in *Research in Photosynthesis, Vol. 1* (Murata, N., Ed.) pp 187–194, Kluwer Academic Publishers, Dordrecht.
Ikegami, I., & Itoh, S. (1988) *Biochim. Biophys. Acta 934*, 39–46.
Jansson, S. (1992) Thesis, University of Umea, Sweden.
Jennings, R. C., Bassi, R., & Zucchelli, G. (1993a) in *Topics in Current Chemistry, Photoinduced Electron Transfer* (Mattay, J., Ed.) Springer, Berlin, New York (in press).
Jennings, R. C., Bassi, R., Garlaschi, F. M., Dainese, P., & Zucchelli, G. (1993b) *Biochemistry 32*, 3203–3210.
Kramer, H. J. M., & Amesz, J. (1982) *Biochim. Biophys. Acta 682*, 201–207.
Kühlbrandt, W., & Wang, D. N. (1991) *Nature 350*, 130–134.
Kwa, S. L. S., Groeneveld, F. G., Dekker, J. P., Van Grondelle, R., Van Amerongen, H., Lin, S., & Struve, W. S. (1992) *Biochim. Biophys. Acta 1101*, 143–146.
Leibl, W., Breton, J., Deprez, J., & Trissl, H. W. (1989) *Photosynth. Res. 22*, 257–275.
Ormos, P., Ansari, A., Braunstein, D., Cowen, B. R., Frauenfelder, H., Hong, M. K., Iben, I. E. T., Sanke, T. B., Steinbach, P. J., & Young, R. D. (1990) *Biophys. J. 57*, 191–199.
Peter, G. F., & Thornber, J. P. (1991) *J. Biol. Chem. 266*, 16745–16754.

Tang, D., Jankowiak, R., Seibert, M., Yocum, C. F., & Small, G. J. (1990) *J. Phys. Chem. 94*, 6519–6522.

Tapie, P., Choquet, Y., Wollman, F.-A., Diner, B. A., & Breton, J. (1986) *Biochim. Biophys. Acta 850*, 156–161.

Trissl, H.-W., Hecks, B., & Wulf, K. (1993) Photochem. Photobiol. 57, 108–112.

Vacha, M., Adamec, F., Ambroz, M., Baumruk, V., Dian, J., Nebdal, L., & Hala, J. (1991) *Photochem. Photobiol. 54*, 127–132.

Van der Vos, R., Carbonera, D., & Hoff, A. J. (1991) *Appl. Magn. Reson. 2*, 197–202.

van Dorssen, R. J., Breton, J., Plijter, J. J., Satoh, K., Van Gorkom, H. J., & Amesz, J. (1987a) *Biochim. Biophys. Acta 893*, 267–274.

van Dorssen, R. J., Plijter, J. J., Dekker, J. P., Den Ouden, A., Amesz, J., & Van Gorkom, H. J. (1987b) *Biochim. Biophys. Acta 890*, 134–143.

Zucchelli, G., Jennings, R. C., & Garlaschi, F. M. (1990) *J. Photochem. Photobiol. B6*, 381–394.

Zucchelli, G., Jennings, R. C., & Garlaschi, F. M. (1992) *Biochim. Biophys. Acta 1099*, 163–169.